

Growth of Fe₃Si/Ge/Fe₃Si trilayers on GaAs(001) using solid-phase epitaxy

S. Gaucher, B. Jenichen,^{a)} J. Kalt, U. Jahn, A. Trampert, and J. Herfort
Paul-Drude-Institut für Festkörperelektronik, Hausvogteiplatz 5-7, 10117 Berlin, Germany

(Received 16 January 2017; accepted 10 February 2017; published online 8 March 2017)

Ferromagnetic Heusler alloys can be used in combination with semiconductors to create spintronic devices. The materials have cubic crystal structures, making it possible to grow lattice-matched heterojunctions by molecular beam epitaxy. However, the development of devices is limited by the difficulty of growing epitaxial semiconductors over metallic surfaces while preventing chemical reactions, a requirement to obtain abrupt interfaces and achieve efficient spin-injection by tunneling. We used a solid-phase epitaxy approach to grow crystalline thin film stacks on GaAs(001) substrates, while preventing interfacial reactions. The crystallized Ge layer forms superlattice regions, which are caused by the migration of Fe and Si atoms into the film. X-ray diffraction and transmission electron microscopy indicate that the trilayers are fully crystalline, lattice-matched, and have ideal interface quality over extended areas. *Published by AIP Publishing.*

[<http://dx.doi.org/10.1063/1.4977833>]

The combination of ferromagnetic Heusler alloys with semiconductors is of great interest for applications in the field of spintronics.^{1,2} The Heusler alloys span a wide range of ferromagnetic compounds, many of which are predicted to be half-metallic.^{3–5} Heusler ferromagnets (FM) have cubic crystal structures that can often be combined with III-V and IV semiconductors (SC), making it possible to create lattice-matched heterojunctions by molecular beam epitaxy (MBE). Heusler alloys have hence been used as spin injection layers to create a variety of devices including spin-transistors^{6,7} and spin-valves.^{8–10} Vertical spin-selective devices made of FM/SC/FM thin film stacks were envisaged recently.^{11–14} However, the realization of such structures remains difficult due to the necessity of overgrowing a metal with a semiconductor by MBE.

Indeed, a longstanding challenge in materials engineering is the growth of epitaxial semiconductors over metals while preserving crystallinity and good interface quality. The difficulty originates from incompatible crystallization energies. Semiconductors require higher growth temperatures at which the bonds of most metals (and Heusler alloys) are susceptible to dissociate, causing chemical reactions and rough interfaces. This technical problem has critical repercussions on device usability. In order to achieve high spin-injection efficiency, the details of the atomic ordering at the interface must be carefully controlled.¹⁵ The conductivity mismatch between Heusler alloys and semiconductors requires transport by tunneling between the layers in order to preserve spin coherence,¹⁶ which is only ensured by a cautious adjustment of the barrier profile.^{17–19} Further evidences show that intermixing and reactions at the FM/SC interface play a significant role on spin transport.^{20–22}

In this work, we studied the possibility to create Fe₃Si/Ge/Fe₃Si thin film stacks on GaAs(001) while preventing interfacial reactions. We used a solid-phase epitaxy (SPE) approach whereby Ge is deposited at low temperature on

ferromagnetic quasi-Heusler compound Fe₃Si and crystallized by annealing, a method that has been successful for other types of semiconductor thin films.^{23,24} The materials chosen are known to have a very small lattice misfit²⁵ (as low as 0.08% for Ge and Fe₃Si). Furthermore, Ge grows crystalline at low temperatures for a semiconductor, which offers better chances of preventing reactions with a metallic substrate during annealing. High quality Fe₃Si has been grown on Ge(111) by MBE,^{26,27} the resulting Schottky barrier could be measured,²⁸ and Fermi level pinning mechanisms were investigated.^{29,30} Spin injection from Fe₃Si to Ge has been demonstrated.³¹ It was shown previously that single crystal Ge films can be grown on Fe₃Si(001) with smooth interface over about 80% of the sample surface at 325 °C, while growing at lower temperatures yields films with very abrupt interfaces but amorphous structures.¹³ FM/SC/FM hybrid trilayers could be grown with a variety of Heusler alloys in combination with Ge and Si in the (111) orientation using surfactant-mediated MBE¹⁴ and low-temperature MBE.^{11,32} However, the (001) orientation is preferable as it is more frequently used for semiconductor technology.

As opposed to MBE direct growth, our SPE approach deposits atoms on a relatively cold substrate. This aspect plays an important role in keeping the metallic surface atomically flat during deposition. Amorphous Ge being already in contact with the smooth underlying Fe₃Si layer, slow annealing ensures the formation of a lattice-matched interface. After determining the optimal annealing temperature, rate, and time, it has then been possible to realize fully crystalline thin film stacks of unprecedented quality in the (001) orientation.

The trilayers are achieved by a combination of low-temperature MBE growth and SPE crystallization. GaAs(001) substrates are first prepared with a 350 nm GaAs buffer layer grown by MBE at 540 °C and As-terminated. The samples are afterwards transferred into a chamber dedicated to metallic compounds, where a film of Fe₃Si is grown at 16 nm/h and 200 °C using well established MBE

^{a)}Electronic mail: bernd.jenichen@pdi-berlin.de

procedures that ensure an abrupt interface with the underlying GaAs substrate.^{25,33} An amorphous layer of Ge is then deposited at 150 °C. Reactions with Fe₃Si were shown to be unlikely at this temperature,¹³ so no byproducts should be created at this stage. To crystallize the amorphous Ge, the samples are heated at 5 °C/min up to temperatures (T_A) between 240 °C and 380 °C and then annealed for 10 min. To obtain the complete layer sequence, a capping Fe₃Si is grown on the crystalline layer using the same growth conditions as for the initial one. The SPE method was tested and shown to be effective for Ge layers with nominal thicknesses ranging from 4 nm to 9 nm. The Fe₃Si layers were grown with various thicknesses between 9 nm and 36 nm.

All steps of the growth were monitored *in situ* by reflected high-energy electron diffraction (RHEED). The surface roughness of the layers was measured by atomic force microscopy (AFM). The thin film stacks were analyzed by X-ray diffraction (XRD) using an X-Pert PRO MRD™ system with a CuK α_1 radiation source at wavelength $\lambda = 1.54056 \text{ \AA}$. The samples were also studied using a transmission electron microscope (TEM), for which they were prepared by mechanical lapping, polishing, and argon ion milling using standard techniques. The TEM system used was a JEOL 3010 operating at 300 kV. Selected area electron diffraction (SAD) capabilities of TEM were used to probe the lattice of the crystallized Ge film. In addition, a JEOL 2100F TEM operating at 200 kV was used for high resolution (HR) imaging. The crystal orientation of the capping Fe₃Si film was investigated by electron backscattered diffraction (EBSD) using a Zeiss ULTRA 55 scanning electron microscope.

The set of adequate annealing parameters was determined by studying the effects of heating on the surface roughness, interface quality and Ge crystallinity. Bilayer samples with 9 nm of amorphous Ge on top of Fe₃Si were annealed at temperatures T_A ranging between 200 °C and 380 °C, using different heating rates (R_H) and times (t_A). The AFM measurements revealed that a slower R_H (i.e., 5 °C/min) is preferable, as it yields smoother Ge surfaces with rms roughness as low as 1 nm. During the annealing, crystallization is indicated by the appearance of streaks in the otherwise foggy RHEED pattern. Such streaks were generally observed starting from 240 °C. In the first 10 min after reaching the desired T_A , the features of the RHEED pattern evolve and generally become clearer, meaning that the Ge crystallinity improves. Annealing for longer t_A did not produce considerable changes in the RHEED and tended to increase surface roughness.

Of all parameters, T_A has the biggest influence on the characteristics of the thin film stacks. XRD was used to track the evolution of the Fe₃Si/Ge interface quality and to reveal the nature of the crystalline compounds formed during annealing. Figs. 1(a) and 1(b) show diffraction curves of multiple Fe₃Si/Ge (9/9) nm samples annealed at 5 °C/min up to different T_A for 10 min. Before annealing, amorphous Ge is invisible as there is no regular lattice for diffraction to occur. The sharp GaAs substrate peaks are superimposed with the Fe₃Si film peaks. The latter show thickness oscillations with a period corresponding to 9 nm. Then, as T_A is increased, other peaks become visible. The curves corresponding to T_A of 240,

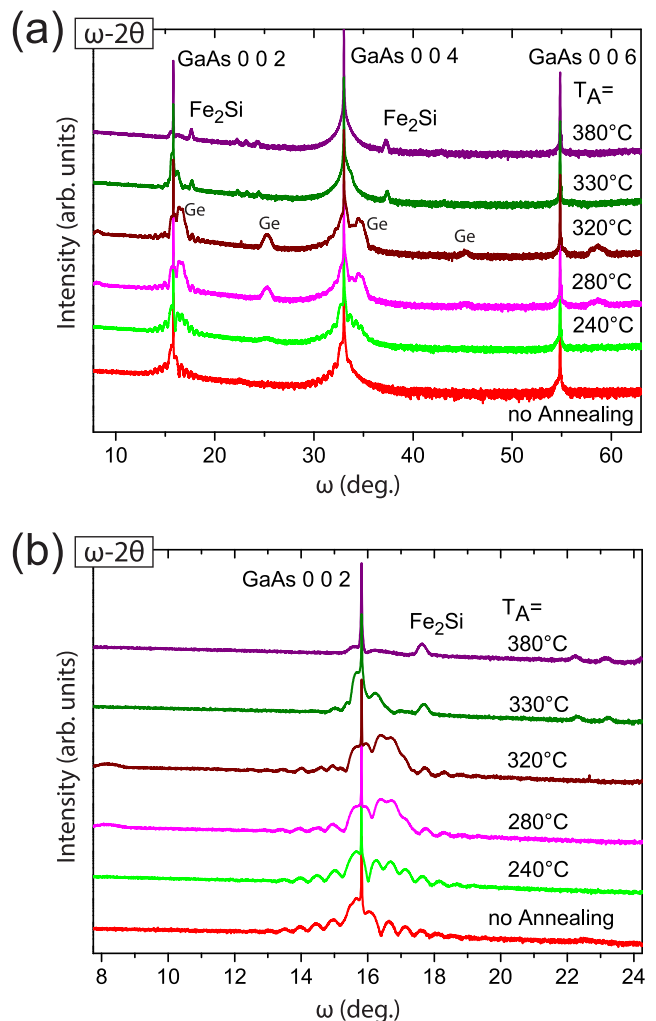


FIG. 1. (a) X-ray diffraction curves of a 9 nm Fe₃Si with 9 nm amorphous Ge annealed at different T_A and (b) detailed view of the curves near the GaAs(002) reflection.

280 and 320 °C contain essentially the same features (although less pronounced for $T_A = 240 \text{ }^\circ\text{C}$). The Fe₃Si film thickness oscillations are preserved, meaning that the interfaces with GaAs and Ge are still abrupt. The crystallization of the amorphous Ge layer is responsible for the emergence of other peaks around 16°, 25°, 35°, 45°, and 57°. As will be discussed, the location of these peaks indicates that the crystallized compound cannot be pure Ge, but rather Ge(Fe,Si). For the sake of clarity, the layer will still be called a Ge layer in the following sections, keeping in mind that it contains some unwanted amount of Fe and Si. Future investigations will aim to reduce diffusion into the Ge film in order to retrieve XRD peaks that coincide with the GaAs substrate peaks. For $T_A \geq 320 \text{ }^\circ\text{C}$, undesired byproducts such as Fe₂Si form at the expense of a single crystalline film. The Fe₃Si thickness oscillations are also suppressed, which further denotes that the interfaces were deteriorated. Based on these results, the best T_A range for the preparation of the trilayers is 240–260 °C.

Figure 2 shows the *in-situ* RHEED images taken after each layer during the growth sequence of a single Fe₃Si/Ge/Fe₃Si sample. The [110] and [010] patterns of both Fe₃Si (1) and (2) layers were observed at the same sample orientations. The main features (position of the streaks, Kikuchi lines) are

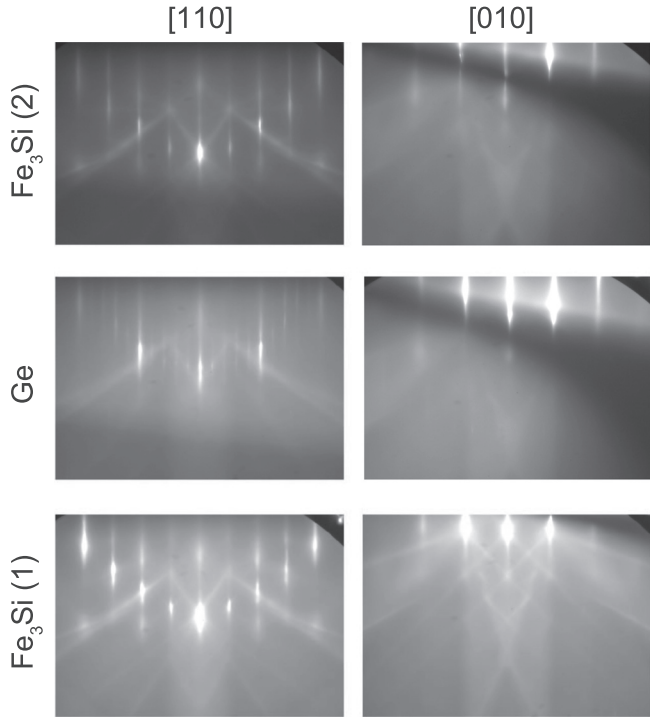


FIG. 2. *In-situ* RHEED patterns along the [110] and [010] azimuths, as observed after growing each layer of the Fe₃Si/Ge/Fe₃Si sample. The Ge layer was annealed at 260 °C for 10 min.

the same and confirm that the structures of the two layers are very similar. The Ge RHEED patterns contain different features, as expected. The important aspect is that the streaks have the same spacing as the Fe_3Si layers in both [110] and [010] orientations, indicating lattice-matched structures and pseudomorphic growth across the whole stack. The clarity of the streaks in the crystallized Ge pattern is also a proof that the SPE yields a high quality film. The presence of Kikuchi lines in all images shows that the surface of the layers remains very flat. Subsequent EBSD characterization (not shown here) confirmed that the top Fe_3Si is indeed single crystalline.

Fig. 3 shows cross-section high resolution (HR) TEM (a), dark-field TEM (b) and SAD (c) images of a trilayer stack with nominal film thicknesses of (36/4/12) nm. The observed Ge thickness is 3 nm. The high resolution STEM micrograph illustrates the superior quality of the films. Once again, one notices that the underlying (36 nm) and capping (12 nm) Fe_3Si layers have the same growth orientation. Both interfaces are sharp and uniform over extended areas (Fig. 3(b)).

In some regions of the samples, as shown in Fig. 3(a), a superlattice forms spontaneously during the crystallization of Ge. The vertical layered structure has a periodicity of about 1 nm, twice the lattice constant of regular diamond cubic Ge. This superlattice is likely caused by the migration of Fe and/or Si atoms during the annealing. Similar superstructures were previously observed in the SiGe epitaxial films.³⁴ However, the mechanism behind the phenomenon depicted in Fig. 3(a) remains unclear. The modification of the lattice is significant and must be caused by a percentage of Fe and Si that goes beyond the doping level, but the exact composition and structure of the compound are still uncertain. So far, the layer is

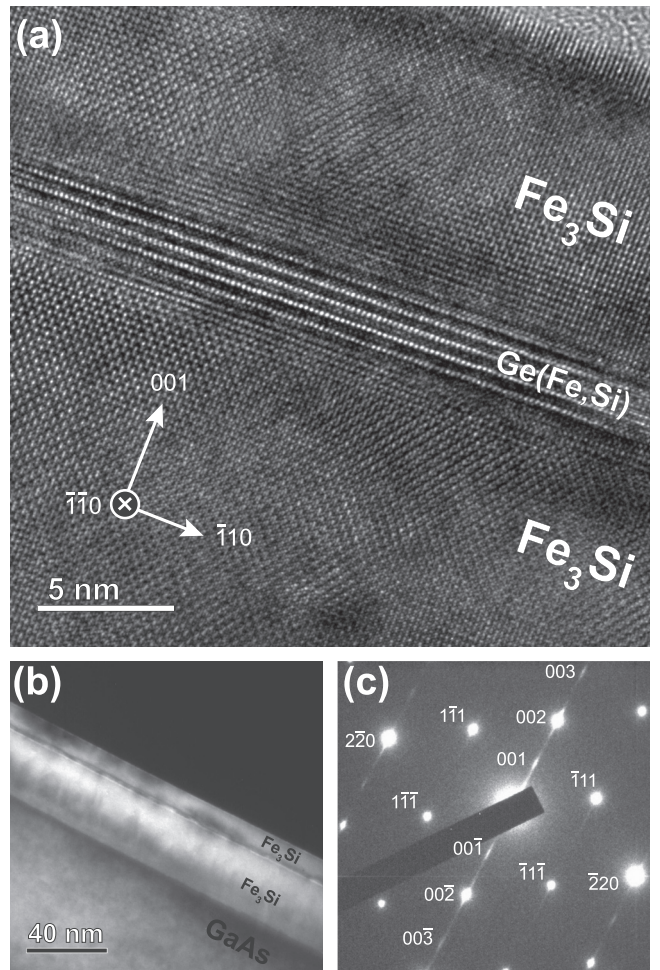


FIG. 3. (a) HR TEM of the Fe₃Si/Ge/Fe₃Si sample with nominal thicknesses of 36/4/12 nm showing fully crystalline layers and Ge(Fe,Si) superlattice phenomenon. In this sample, the Ge layer was annealed at 240 °C for 10 min. Here, the observed Ge film thickness is 3 nm. (b) Dark field TEM micrograph of the same sample showing abrupt interfaces over extended areas. (c) SAD pattern of the Ge(Fe,Si) layer with faint odd integer reflection spots (001, 00̄1, 003 and 00̄3) caused by the superlattice structure.

regarded as a Ge(Fe,Si) single crystal, where the Fe and/or Si atoms sit on regular lattice sites. The migration of Fe and Si into the Ge film leads to tetragonal deformation of the originally cubic Ge, as visible in the XRD curves of Fig. 1. The Ge(002) and (004) reflection peaks are displaced to higher angles by about 1° – 2° , indicating that the crystallized compound has a smaller lattice spacing. Furthermore, the satellite peaks appear between the Ge(002*n*) reflections at angles that are generally forbidden for diamond structures. The SAD pattern shown in Fig. 3(c) provides an additional evidence for a single crystalline film. The satellite peaks caused by the super-lattice are also visible as faint spots labeled 001, 001̄, 003, and 003̄.

Fig. 4 illustrates the effect of adding the top Fe₃Si layer on the XRD diffraction curves, as well as the contribution from Ge layers of different nominal thicknesses. The lower curve (red) corresponds to a bilayer of Fe₃Si/Ge (36/4) nm similar to the one shown in Figs. 1(a) and 1(b), while the upper ones are trilayered stacks all annealed at 240 °C but with different Ge layer thicknesses. The Ge film produces

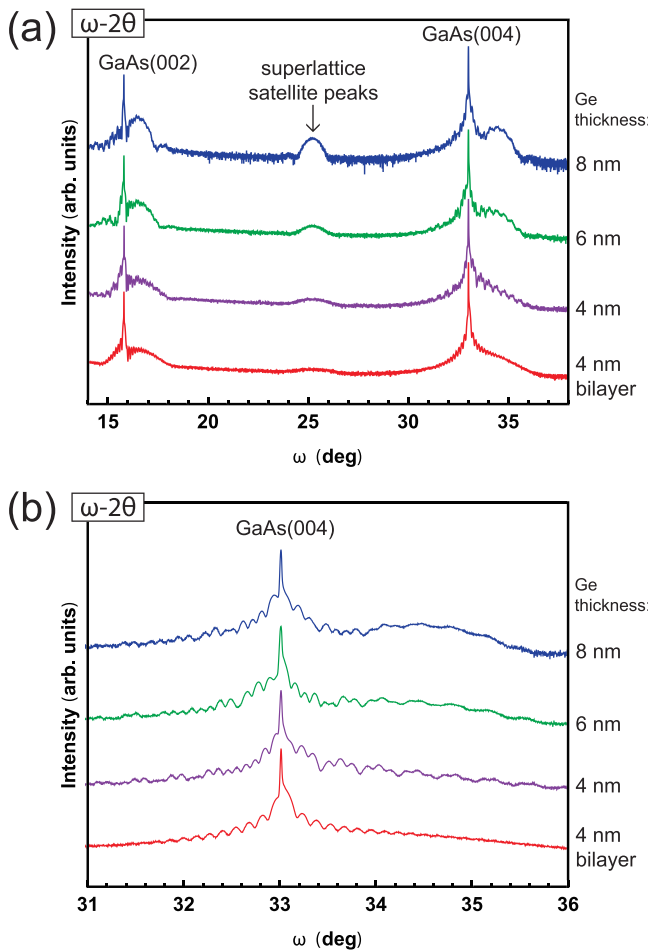


FIG. 4. (a) X-ray diffraction curves of the Fe_3Si (36 nm)/Ge bilayer (red) and $\text{Fe}_3\text{Si}/\text{Ge}/\text{Fe}_3\text{Si}$ (12 nm) trilayers with different Ge thickness, all annealed at 240 °C and (b) detailed view of the curves about the GaAs(004) reflection.

the three broader peaks, two of which exhibiting Fe_3Si film thickness oscillations (about the GaAs(002) and (004) reflections). The satellite peak associated with the superlattice (at $\omega \approx 25^\circ$) cannot carry Fe_3Si oscillations, as this reflection is usually forbidden for cubic Fe_3Si (e.g., B2 structure). The Ge is itself too thin to generate visible oscillations. However, as the films get thicker, the intensity of the peaks increases while their width reduces. This correlation establishes a clear link between the three peaks and the crystallized Ge layer. The stacks have well-defined $\text{Fe}_3\text{Si}/\text{Ge}$ interfaces as seen from the number of Fe_3Si film thickness oscillations. The addition of the capping Fe_3Si layer creates a beating pattern in the diffraction curves. The 36 and 12 nm films produce oscillations with periods in a ratio 1:3, inversely proportional to their respective thicknesses. The XRD curves are effectively a convolution of the individual film contributions. The possibility to resolve the films in this way confirms that the SPE approach yields ideal abrupt interfaces over the whole area of the samples.

Fully crystalline $\text{Fe}_3\text{Si}/\text{Ge}/\text{Fe}_3\text{Si}$ thin film stacks with ideal interface quality were grown. SPE was used as a solution to grow crystalline Ge on top of metal Fe_3Si . The fact that Ge was deposited at low temperature helped to keep the Fe_3Si surface atomically flat, which played an important role in the

creation of a sharp interface during annealing. The superior nature of the films was revealed by their individual contributions to the XRD curves. STEM and RHEED showed that the films are lattice-matched single crystals with pristine interfaces. The crystallized Ge layer forms superlattice-regions causing satellite peaks. The migration of Fe and Si atoms is probably responsible for this lattice modification. The resulting $\text{Ge}(\text{Fe},\text{Si})$ is however a single crystal; otherwise, the capping Fe_3Si could not be grown with such high quality while preserving lattice orientation. The SPE approach is therefore a convenient tool to explore the combination of ferromagnetic Heusler alloys with semiconductors in the FM/SC/FM configuration, a step towards the implementation of vertical spintronic devices.

The authors thank C. Herrmann and H.-P. Schönher for their valuable support during the growth of the samples as well as S. Krauss and M. Matzek for the preparation of the TEM specimens.

- ¹C. J. Palmstrøm, *MRS Bull.* **28**, 725 (2003).
- ²C. J. Palmstrøm, *Prog. Cryst. Growth Charact. Mater.* **62**, 371 (2016).
- ³R. A. de Groot, F. M. Mueller, P. G. van Engen, and K. H. J. Buschow, *Phys. Rev. Lett.* **50**, 2024 (1983).
- ⁴T. Block, M. J. Carey, B. A. Gurney, and O. Jepsen, *Phys. Rev. B* **70**, 205114 (2004).
- ⁵*Lecture Notes in Physics*, edited by I. Galanakis and P. H. Dederichs (Springer, Berlin, Heidelberg, 2005), Vol. 676.
- ⁶Y. Ohdaira, M. Oogane, H. Naganuma, and Y. Ando, *Appl. Phys. Lett.* **99**, 132513 (2011).
- ⁷S. Sugahara and M. Tanaka, *Appl. Phys. Lett.* **84**, 2307 (2004).
- ⁸Y. Ando, K. Kasahara, K. Yamane, K. Hamaya, K. Sawano, T. Kimura, and M. Miyao, *Appl. Phys. Express* **3**, 093001 (2010).
- ⁹Y. Manzke, R. Farshchi, P. Bruski, J. Herfort, and M. Ramsteiner, *Phys. Rev. B* **87**, 134415 (2013).
- ¹⁰P. Bruski, Y. Manzke, R. Farshchi, O. Brandt, J. Herfort, and M. Ramsteiner, *Appl. Phys. Lett.* **103**, 052406 (2013).
- ¹¹S. Yamada, K. Tanikawa, M. Miyao, and K. Hamaya, *Cryst. Growth Des.* **12**, 4703 (2012).
- ¹²I. Maafa, S. Hajjar-Garreau, R. Jaafar, D. Berling, C. Pirri, A. Mehdaoui, E. Denys, A. Florentin, and G. Garreau, *J. Phys.: Condens. Matter* **25**, 256007 (2013).
- ¹³B. Jenichen, J. Herfort, U. Jahn, A. Trampert, and H. Riechert, *Thin Solid Films* **556**, 120 (2014).
- ¹⁴M. Kawano, M. Ikawa, K. Arima, S. Yamada, T. Kanashima, and K. Hamaya, *J. Appl. Phys.* **119**, 045302 (2016).
- ¹⁵B. D. Schultz, N. Marom, D. Naveh, X. Lou, C. Adelmann, J. Strand, P. A. Crowell, L. Kronik, and C. J. Palmstrøm, *Phys. Rev. B* **80**, 201309 (2009).
- ¹⁶E. I. Rashba, *Phys. Rev. B* **62**, R16267 (2000).
- ¹⁷A. T. Hanbicki, B. T. Jonker, G. Itsos, G. Kioseoglou, and A. Petrou, *Appl. Phys. Lett.* **80**, 1240 (2002).
- ¹⁸A. T. Hanbicki, O. M. J. van't Erve, R. Magno, G. Kioseoglou, C. H. Li, B. T. Jonker, G. Itsos, R. Mallory, M. Yasar, and A. Petrou, *Appl. Phys. Lett.* **82**, 4092 (2003).
- ¹⁹Q. O. Hu, E. S. Garlid, P. A. Crowell, and C. J. Palmstrøm, *Phys. Rev. B* **84**, 085306 (2011).
- ²⁰C. Adelmann, B. D. Schultz, X. Y. Dong, C. J. Palmstrom, X. Lou, J. Strand, J. Q. Xie, S. Park, M. R. Fitzsimmons, and P. A. Crowell, in *16th IPRM, 2004 International Conference on Indium Phosphide and Related Materials, 2004* (Kagoshima, Japan, 2004), p. 505.
- ²¹T. J. Zega, A. T. Hanbicki, S. C. Erwin, I. Žutić, G. Kioseoglou, C. H. Li, B. T. Jonker, and R. M. Stroud, *Phys. Rev. Lett.* **96**, 196101 (2006).
- ²²D. O. Demchenko and A. Y. Liu, *Phys. Rev. B* **73**, 115332 (2006).
- ²³R. Hey, P. Santos, E. Luna, T. Flissikowski, and U. Jahn, *J. Cryst. Growth* **323**, 5 (2011).
- ²⁴E. Luna, R. Hey, and A. Trampert, *J. Vac. Sci. Technol. B* **30**, 02B108 (2012).
- ²⁵J. Herfort, H.-P. Schönher, and K. H. Ploog, *Appl. Phys. Lett.* **83**, 3912 (2003).

- ²⁶Y. Ando, K. Hamaya, K. Kasahara, K. Ueda, Y. Nozaki, T. Sadoh, Y. Maeda, K. Matsuyama, and M. Miyao, *J. Appl. Phys.* **105**, 07B102 (2009).
- ²⁷K. Hamaya, T. Murakami, S. Yamada, K. Mibu, and M. Miyao, *Phys. Rev. B* **83**, 144411 (2011).
- ²⁸M. Miyao, K. Hamaya, K. Sadoh, H. Itoh, and Y. Maeda, *Thin Solid Films* **518**, S273 (2010).
- ²⁹K. Yamane, K. Hamaya, Y. Ando, Y. Enomoto, K. Yamamoto, T. Sadoh, and M. Miyao, *Appl. Phys. Lett.* **96**, 162104 (2010).
- ³⁰K. Kasahara, S. Yamada, K. Sawano, M. Miyao, and K. Hamaya, *Phys. Rev. B* **84**, 205301 (2011).
- ³¹M. Kawano, K. Santo, M. Ikawa, S. Yamada, T. Kanashima, and K. Hamaya, *Appl. Phys. Lett.* **109**, 022406 (2016).
- ³²K. Hamaya, M. Kawano, Y. Fujita, S. Oki, and S. Yamada, *Materials Transactions* **57**, 760 (2016).
- ³³J. Herfort, H.-P. Schönherr, K.-J. Friedland, and K. H. Ploog, *J. Vac. Sci. Technol. B* **22**, 2073 (2004).
- ³⁴A. Ourmazd and J. C. Bean, *Phys. Rev. Lett.* **55**, 765 (1985).